



Supplement of

Validation of formaldehyde products from three satellite retrievals (OMI SAO, OMPS-NPP SAO, and OMI BIRA) in the marine atmosphere with four seasons of Atmospheric Tomography Mission (ATom) aircraft observations

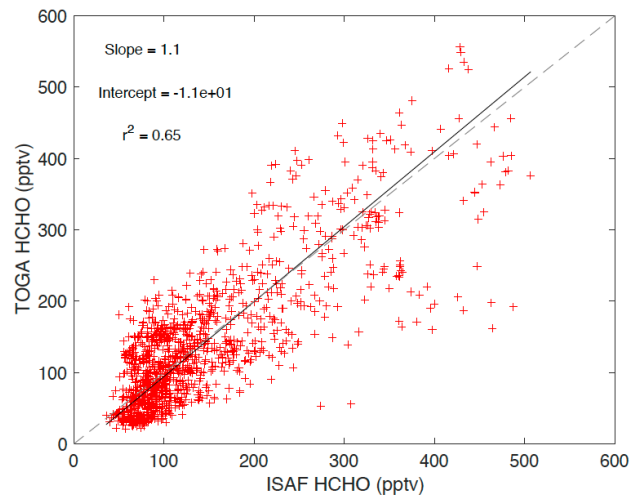
Jin Liao et al.

Correspondence to: Jin Liao (jin.liao@nasa.gov)

The copyright of individual parts of the supplement might differ from the article licence.

1

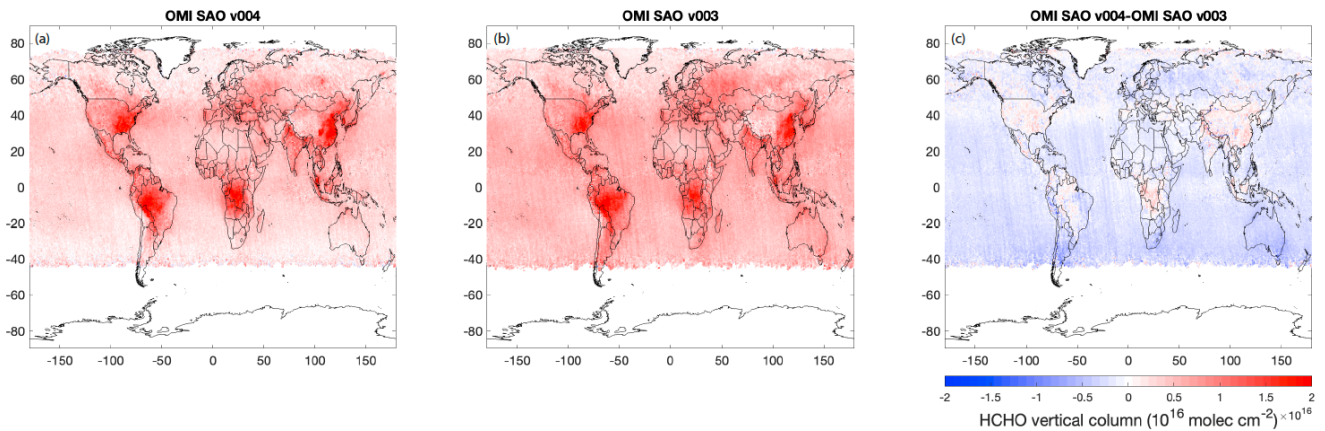
Supplementary Information



2

3 **Figure S1. TOGA HCHO measurements vs. ISAF HCHO measurements during ATom-4 over oceans. Equally**
4 **weighted linear regression yields a slope of 1.1 and an intercept of -11. The correlation coefficient $r^2 = 0.65$.**

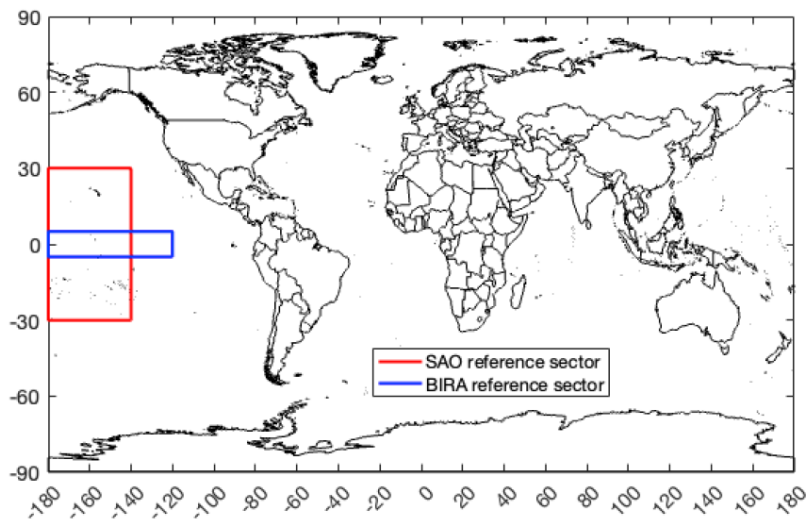
5



6

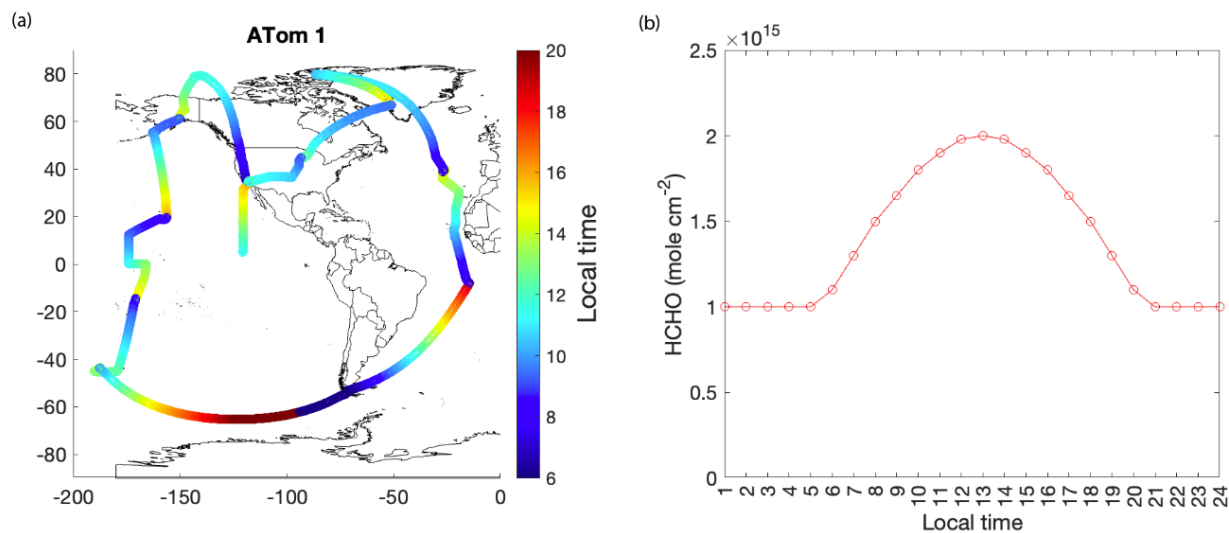
7

8 **Figure S2. Global map of average HCHO vertical column over ATom-1 sampling period for (a) OMI SAO (v004), (b)**
9 **OMI SAO (v003), and (c) their differences.**



10
11
12
13
14
15
16
17
18

Figure S3. Map of the approximate reference sector locations in SAO and BIRA retrievals for reference spectrum and background HCHO addition. The SAO retrieval reference sector location slightly varies depending on the locations of the closest satellite crossing.



19
20
21
22
23
24
25

Figure S4. (a) Map of ATom1 flight track color-coded with local time. ATom 2, 3, and 4 maps are similar to ATom1 and not shown here. (b) Diurnal variation of HCHO columns with maximum value of 2.0×10^{15} molec cm^{-2} at 1: 00 pm is simulated, as an example. The diurnal variation is based on the profiles from Bruno Franco et al. (2016) and the maximum value is selected based on average satellite HCHO measurements at the northern high latitudes. It is important to note that the diurnal variation shown in (b) likely represents the upper limit of diurnal HCHO column fluctuations in the remote oceanic atmosphere, especially in the high latitudes, as suggested by the measurements

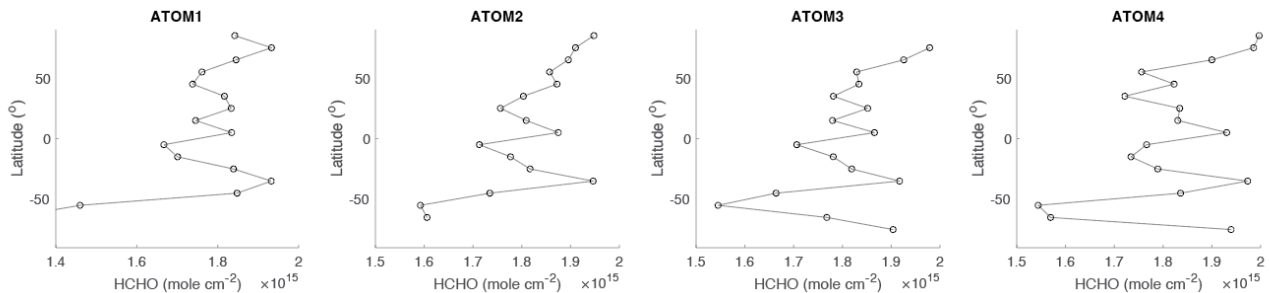
26 reported in Vigouroux et al. (2018).

27

28

29

30

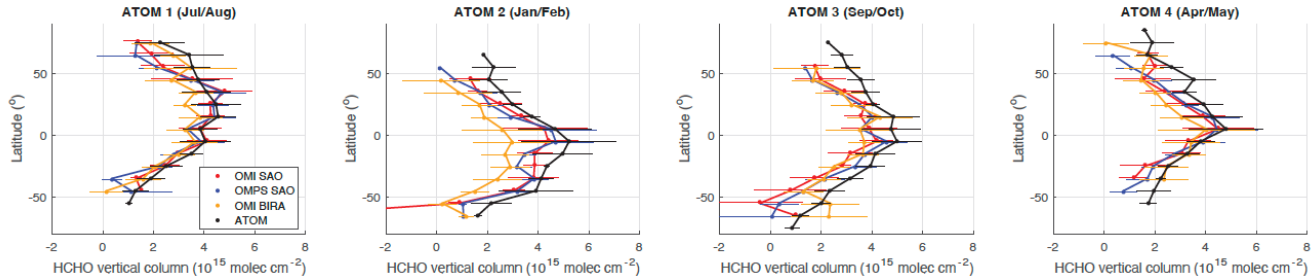


31

32 **Figure 5S. The latitude-averaged distribution of simulated HCHO columns, using HCHO columns as a function of local**
33 **time (Figure S4b) and the local time of the ATom flight tracks. This figure highlights the differences between satellite**
34 **and ATom measurements across latitudes, which arise solely from the time discrepancies-- 1:30 pm local time for**
35 **satellite measurements and varying local times for ATom measurements (Figure S4a). When comparing these**
36 **measurements across latitudes, ATom measurements may appear higher than satellite measurements at higher latitudes**
37 **(e.g., ATom1 70° N compared to 30° N in Figure 5S) due to local time differences. However, the local time effect**
38 **contributing about 0.2×10^{15} molec cm⁻², is relatively minor compared to the overall differences between satellite and**
39 **ATom measurements across latitudes (e.g., Figure 2 ATom1 70° N vs. 30° N). The relatively large variation in high**
40 **southern latitudes may suggest that the simulated HCHO column variability is significantly overestimated for this**
41 **region.**

42

43



44

45 **Figure 6S. Area weighted HCHO column density from three satellite retrievals (OMI SAO in red, OMPS SAO in blue, and OMI**
46 **BIRA in orange) and ATom in situ measurements (black) at different latitudes. The dots represent the averaged column density for**
47 **$\pm 5^\circ$ latitude bins and the bars are the standard deviation within the latitude bin. OMI SAO error bars are vertically offset for clarity.**

48

49

50 Molecule number concentration is calculated by Eq.(S1)

$$51 M = N_a \times P / R / T \quad (S1)$$

52 Where N_a is Avogadro's number 6.022×10^{23} mol⁻¹; P is pressure in mbar; R is gas constant 8.314×10^4 cm³ mbar K⁻¹ mol⁻¹ and

53 T is temperature in K.

54

55 References:

56

57 Franco, B., Marais, E. A., Bovy, B., Bader, W., Lejeune, B., Roland, G., Servais, C., and Mahieu, E.: Diurnal cycle and multi-
58 decadal trend of formaldehyde in the remote atmosphere near 46°N, *Atmos. Chem. Phys.*, 16, 4171–4189,
59 <https://doi.org/10.5194/acp-16-4171-2016>, 2016.

60

61 Vigouroux, C., Bauer Aquino, C. A., Bauwens, M., Becker, C., Blumenstock, T., De Mazière, M., García, O., Grutter, M.,
62 Guarin, C., Hannigan, J., Hase, F., Jones, N., Kivi, R., Koshelev, D., Langerock, B., Lutsch, E., Makarova, M., Metzger, J.-M.,
63 Müller, J.-F., Notholt, J., Ortega, I., Palm, M., Paton-Walsh, C., Poberovskii, A., Rettinger, M., Robinson, J., Smale, D.,
64 Stavrakou, T., Stremme, W., Strong, K., Sussmann, R., Té, Y., and Toon, G.: NDACC harmonized formaldehyde time series
65 from 21 FTIR stations covering a wide range of column abundances, *Atmos. Meas. Tech.*, 11, 5049–5073,
66 <https://doi.org/10.5194/amt-11-5049-2018>, 2018.

67